

Computed Tomography–based Measurement of Herniated Orbital Volume Following Acute Orbital Fractures

Erina Kawabata, MD*
Takashi Nuri, MD, PhD*
Tatsuya Ichida, MD†
Koichi Ueda, MD, PhD*

Background: To predict which patients will develop more than 2 mm of enophthalmos and require surgery after orbital fracture is challenging. Although high herniated orbital volume (HV) might be a predictor, its measurement can be complex and time-consuming. This study aimed to identify a simple, reliable, and clinically applicable method for measuring herniated orbital volume.

Methods: This single-center retrospective study examined HV and approximate volume in 42 patients with an orbital floor fracture (OF group) and 56 patients with a medial wall fracture (MW group). Approximate herniated volume (AV) was calculated as a rectangular parallelepiped, quadrangular pyramid, or hemiellipsoid. The correlation between HV and AV was analyzed quantitatively. Receiver operating characteristic curve analysis was performed to compare AV and HV cutoff values.

Results: AV calculated as a hemiellipsoid (AVhe) provided the closest approximation to HV. Correlation analysis showed a positive linear relationship between HV and AVhe in both the OF group ($r=0.818$) and the MW group ($r=0.84$). The optimal AVhe cutoff value was 1.013 mL in the OF group (positive and negative predictive values, 96.3% and 66.7%, respectively; area under the curve, 0.925) and 1.13 mL in the MW group (positive and negative predictive values, 90.0% and 69.2%, respectively; area under the curve, 0.956). High HV was defined as greater than 1.0 mL in the OF group and greater than 0.9 mL in the MW group.

Conclusions: A simplified method that approximately calculates the volume of herniated orbital contents in a hemiellipsoid pattern model proved to be practical, easy, and reliable. (*Plast Reconstr Surg Glob Open* 2025;13:e6689; doi: [10.1097/GOX.00000000000006689](https://doi.org/10.1097/GOX.00000000000006689); Published online 16 April 2025.)

INTRODUCTION

Early repair of orbital fractures and repositioning of any herniated orbital contents are crucial to prevent impairment of the field of vision and eye movement.¹ Delayed repair can be technically challenging owing to the development of fibrosis and may increase the risk of unsatisfactory results.²

Persistent diplopia, posttraumatic enophthalmos (PE), and orbital content entrapment are established

indications for surgical repair.^{3–6} More than 2 mm of PE can cause cosmetic and functional morbidity and is generally considered clinically significant.^{4,7–15} However, post-traumatic orbital edema and periocular swelling may cause the development of PE to be delayed until the ideal period for surgical intervention has passed.^{16,17} Therefore, surgical decision-making regarding orbital fractures early after the injury can be difficult.

Estimating which patients will develop more than 2 mm of PE and require surgery can optimize treatment outcomes by minimizing the risks associated with unnecessary or delayed intervention.¹⁸ Previous studies have attempted to clarify the correlation between the degree of PE and several anatomic parameters present on computed tomography (CT) at the time of injury. In a systematic review, 5 factors influenced the development of delayed PE: orbital defect height and width, involvement of specific intraorbital structures, rounding of the inferior rectus muscle, orbital fracture area, and volumetric analysis stratified by fracture site.¹⁹ Several studies have

From the *Department of Plastic and Reconstructive Surgery, Osaka Medical and Pharmaceutical University, Takatsuki, Osaka, Japan; and †Department of Plastic Surgery, Ueyama Hospital, Neyagawa, Osaka, Japan.

Received for publication September 4, 2024; accepted February 20, 2025.

Copyright © 2025 The Authors. Published by Wolters Kluwer Health, Inc. on behalf of The American Society of Plastic Surgeons. This is an open-access article distributed under the terms of the [Creative Commons Attribution-Non Commercial-No Derivatives License 4.0 \(CCBY-NC-ND\)](https://creativecommons.org/licenses/by-nc-nd/4.0/), where it is permissible to download and share the work provided it is properly cited. The work cannot be changed in any way or used commercially without permission from the journal.

DOI: [10.1097/GOX.00000000000006689](https://doi.org/10.1097/GOX.00000000000006689)

Disclosure statements are at the end of this article, following the correspondence information.

incorporated these parameters into predictive algorithms used as clinical tools.^{18,20,21} Herniated orbital volume (HV) is frequently incorporated into these algorithms. However, HV measurement can be complex and time-consuming, as it requires meticulous manual tracing of intricate borders. Moreover, the thinner the CT slice, the more layers need to be traced.²⁰

This study aimed to identify a simple yet reliable method for measuring HV. We hypothesized that an approximate volume, calculated by measuring only 3 dimensions on CT, could replace the conventional method of tracing borders in great detail. The shapes of the approximate volumes were compared and analyzed as rectangular parallelepiped, quadrangular pyramid, or hemiellipsoid.

MATERIALS AND METHODS

Patients

All patients with orbital fractures who were treated by the plastic and reconstructive surgery department in our institution between January 2008 and June 2021 were retrospectively reviewed. Patients who did not undergo initial facial bone CT within 1 week of injury and those with bilateral orbital fractures, lateral orbital wall fractures, orbital roof fractures, inferomedial orbital fractures, fractures of the inferomedial buttress, and linear orbital fractures were excluded. We also excluded patients with concomitant midfacial fractures other than nasal bone fractures. None of the study patients had a history of orbital injury, orbital surgery, or congenital craniofacial anomaly.

The study was approved by the institutional review board of our medical center (No. 2023-047). The requirement for written informed consent was waived owing to its retrospective nature.

Data Collection

Patient data, including age, sex, cause of injury, laterality of injury, fracture location, and the interval between injury and initial facial bone CT were collected from the electronic medical record (Fujifilm Medical Co., Ltd., Tokyo, Japan).

CT Findings

Facial bone CT (slice thickness ≤ 3 mm) was reviewed using standard bone and soft-tissue windows to assess HV and other parameters. All parameters were measured 3 times by a single plastic surgeon using Synapse software (Fujifilm Medical Co., Ltd.); parameter mean values were calculated for analysis. Patients were grouped according to fracture location: orbital floor (OF) and medial wall (MW).

In the OF group, the maximum length of the fracture line on coronal and sagittal CT views was denoted as X and Y , respectively; in the MW group, the maximum length on coronal and axial CT views was denoted as X and Y , respectively. In both groups, the maximum distance that the fractured part was displaced was measured on a coronal view and designated as Z (Figs. 1, 2).

Takeaways

Question: The purpose of this study is to identify a simple, reliable, and clinically applicable method for measuring herniated orbital volume in patients with orbital fractures.

Findings: This study analyzed clinical data, including herniated orbital volume and approximate herniated volume, as determined by computed tomography, in 42 patients with orbital floor fractures and 56 patients with medial wall fractures. Approximate herniated volume calculated as a hemiellipsoid provided the closest approximation to herniated orbital volume.

Meaning: The simplified method using approximate volume calculated as a hemiellipsoid proved to be more practical, easier, and more reliable than conventional methods.

Herniated orbital tissue was defined as soft tissue that extended beyond the normal orbital boundaries into the maxillary or ethmoid sinuses and was manually outlined on coronal views. The cross-sectional areas of the herniated tissue on each coronal slice were summed and multiplied by the slice thickness to determine HV. The approximate herniated volume (AV) was calculated using 3 different shape assumptions: rectangular parallelepiped (AVrp) was calculated as XYZ , quadrangular pyramid (AVqp) as $XYZ/3$, and hemiellipsoid (AVhe) as $\pi XYZ/6$ (Figs. 1, 2).

Statistical Methods

Statistical analyses were conducted using EZR on R Commander version 1.52 (Jichi Medical University, Saitama, Japan).²² Categorical variables are expressed as numbers with percentages and were compared using the Fisher exact test. Continuous variables are presented as means with SD. Two-group comparisons of continuous data were performed using the Student t test. Three-group comparisons were performed using analysis of variance; if a significant P value was found, the Student t test was then used to identify which specific group pairings exhibited a significant difference. Correlation was assessed using the Pearson method.

Receiver operating characteristic (ROC) curve analysis was performed to compare the AV and HV cutoff values, as high HV had been associated with PE of 2 mm or more. Based on previous studies,^{13,23,24} high HV was defined as greater than 1.0 mL in the OF group and greater than 0.9 mL in the MW group. The area under the ROC curve (AUC) was calculated as a measure of predictive performance, which was categorized as follows: AUC 0.5–0.6, failure; AUC 0.6–0.7, poor; AUC 0.7–0.8, fair; AUC 0.8–0.9, good, and AUC 0.9–1.0, excellent. The optimal cutoff value was selected to maximize the sum of sensitivity and specificity. A P value less than 0.05 was considered significant.

RESULTS

Of the 330 patients with orbital fractures identified during the study period, 89 were excluded because of

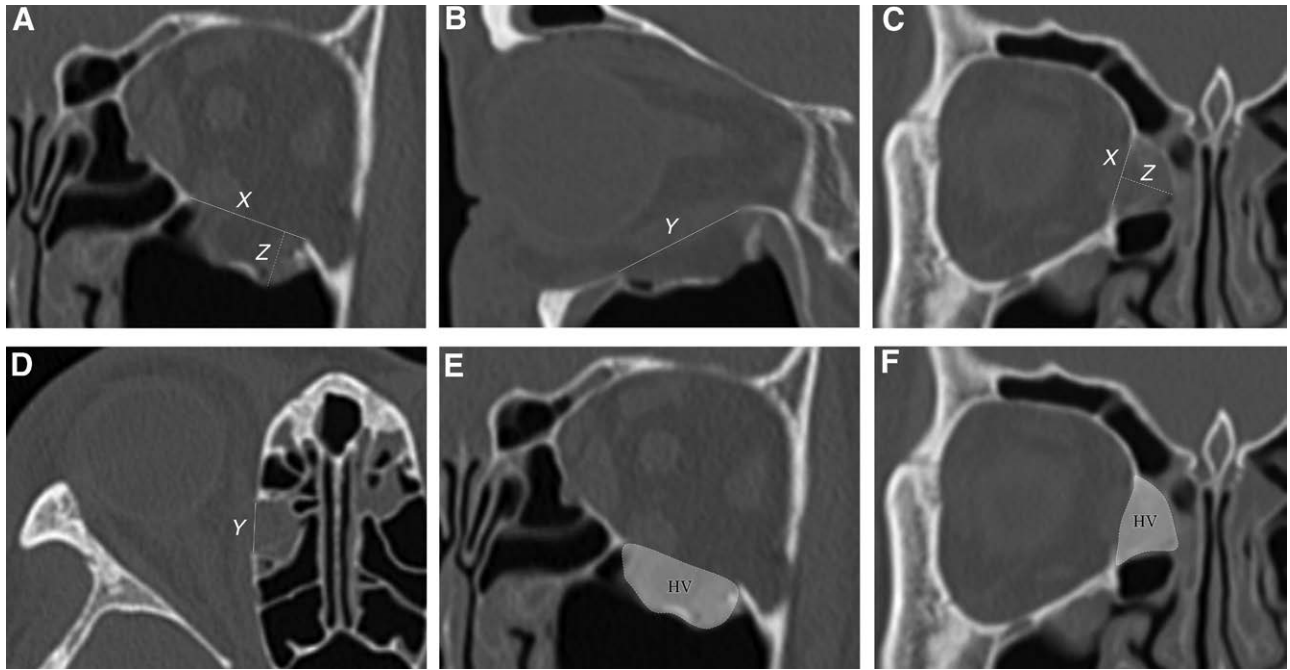


Fig. 1. Measurement of CT parameters and HV. A and B, OF fracture. Coronal and sagittal sections were used to define X and Y as the maximum length of the bone defect. On the coronal section, Z was established as the maximum distance the fractured portion moved. C and D, MW orbital fracture. Coronal and axial sections were used to determine X and Y, and Z was determined on the coronal section. E and F, The herniated volume was traced on each coronal slice (dashed line and labeled “HV”).

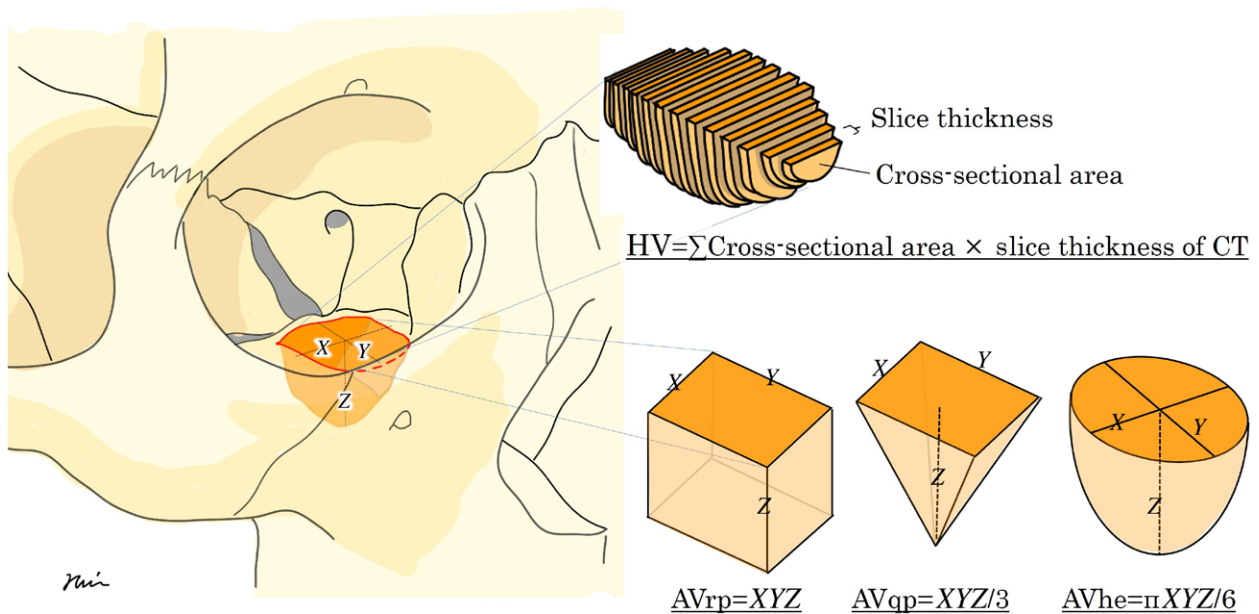


Fig. 2. HV and AV. XYZ in the schema corresponds to XYZ in the CT parameters.

other facial bone trauma. Among the remaining 241, the most frequent fracture location was the OF (n = 129; 53.5%), followed by the MW (n = 76; 31.5%). The primary mechanisms of injury included sports-related incidents (n = 49; 20.3%), falls (n = 35; 14.5%), and traffic accidents (n = 24; 10.0%).

A total of 143 patients were excluded because their initial CT images were not available (n = 96) or they had sustained bilateral orbital fractures, orbital roof fractures, inferomedial orbital fractures, or linear orbital fractures (n = 47). Finally, 98 patients were included for analysis. Mean age was 42.3 ± 22.5 years (range, 13–89 y).

The cohort comprised 68 men (69.4%) and 30 women (30.6%). The laterality of fracture was right in 50 patients (51.0%). Sixteen patients underwent operative management (16.3%). The OF group consisted of 42 (42.9%) patients and the MW group comprised 56 (57.1%). Patient characteristics are summarized in Table 1. In the OF group, the mean HV was 2.03 ± 1.38 mL, the mean AVrp was 2.9 ± 1.90 mL, the mean AVqp was 0.97 ± 0.63 mL, and the mean AVhe was 1.52 ± 1.00 mL. The corresponding mean volumes in the MW group were 1.40 ± 1.38 , 2.29 ± 1.78 , 0.76 ± 0.59 , and 1.48 ± 1.33 mL, respectively.

To determine which approximate volume shape best approximates the actual hernia volume, we calculated the difference between HV and AVrp/AVqp/AVhe. In the OF group, the mean HV–AVrp difference was 1.11 ± 0.88 mL, the mean HV–AVqp difference was 1.07 ± 0.94 mL, and the mean HV–AVhe difference was 0.62 ± 0.73 mL; the differences in mean values were significant in the analysis of variance ($P = 0.016$). The corresponding mean differences in the MW group were

0.97 ± 0.89 , 0.65 ± 0.93 , and 0.54 ± 0.83 mL, respectively; these mean differences were also significantly different ($P = 0.032$).

The direct comparisons of mean differences in the OF and MW groups are shown in Figure 3. In the OF group, the mean HV–AVhe difference significantly differed from both the mean HV–AVhrp difference ($P = 0.006$) and the mean HV–AVqp difference ($P = 0.018$); the difference between the mean HV–AVhrp difference and the mean HV–AVqp difference was not significant ($P = 0.81$). In the MW group, only the difference between the HV–AVhrp mean difference and the HV–AVhe mean difference was significant ($P = 0.01$).

Scatterplots with the Pearson correlation analysis of HV and AVhe in the OF and MW groups are shown in Figure 4. Correlation analysis showed a positive linear relationship between HV and AVhe in both the OF group ($r = 0.818$; $P < 0.001$) and the MW group ($r = 0.846$; $P < 0.001$).

Tables 2 and 3 show the comparison of the high and low HV subgroups in both the OF group (Table 2) and the MW group (Table 3). Age, sex, and fracture laterality did not significantly differ between the high and low HV subgroups in the OF group. In the MW group, age and sex did not significantly differ between the subgroups but fracture site laterality did ($P = 0.011$). These findings suggest that the high and low HV subgroups in each group were fairly similar.

ROC curves for the association of AVhe with high HV in the OF group (HV > 1.0 mL) and MW group (HV > 0.9 mL) are shown in Figure 5. The optimal AVhe cutoff value in the OF group was 1.013 mL (sensitivity of 83.9%, specificity of 90.9%, positive predictive value of 96.3%, negative predictive value of 66.7%, and AUC of 0.925 [95% confidence interval, 0.848–1]). In the MW group, the optimal AVhe cutoff value for predicting high HV was 1.13 mL (sensitivity of 77.1%, specificity of 100%, positive predictive value of 90.0%, negative predictive value of

Table 1. Patient Characteristics

Characteristics of Analysis Population	
Sample size	98
OF, n (%)	42 (42.9)
MW, n (%)	56 (57.1)
Age, mean \pm SD, y	42.3 \pm 22.5
Sex, n (%)	
Men	68 (69.4)
Women	30 (30.6)
Fractures site, n (%)	
Right	50 (51.0)
Left	48 (49.0)
Treatment, n (%)	
Surgical repair	16 (16.3)
Conservative	82 (83.7)

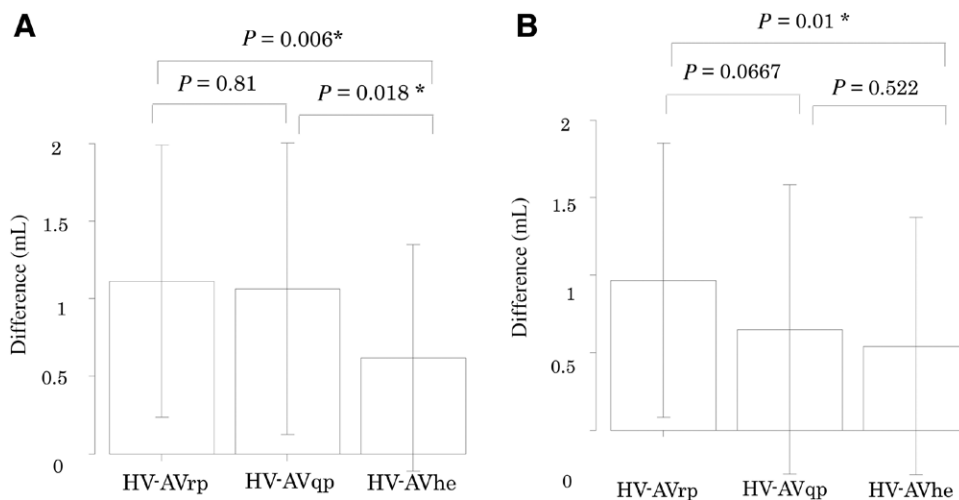


Fig. 3. Comparison of the differences between herniated orbital tissue and approximated herniated orbital tissue volumes in the (A) OF fracture group and (B) MW fracture group. Bars show means \pm standard error. *Statistically significant ($P < 0.05$).

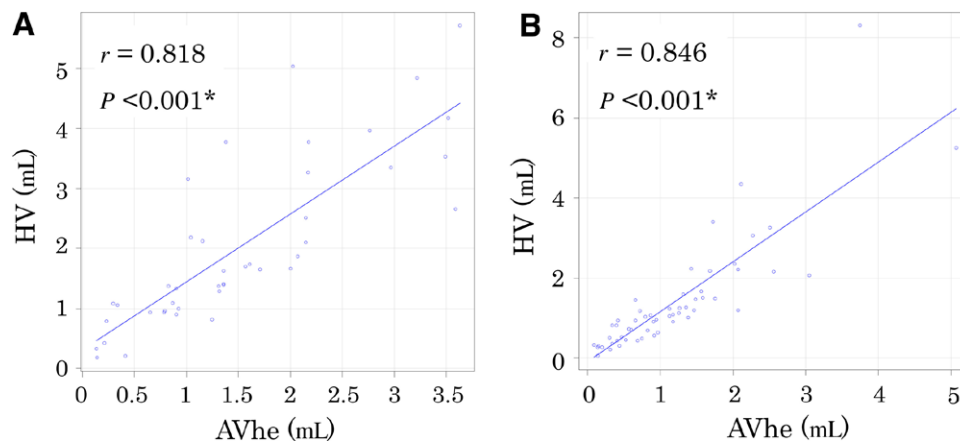


Fig. 4. Correlation between the degree of HV and volume approximated by assuming a hemiellipsoid shape in the (A) OF fracture group and (B) MW fracture group. *Statistically significant ($P < 0.05$).

Table 2. Bivariate Analysis of All Study Variables Versus the Volume of Herniated Orbital Tissue in the Orbital Wall Fracture Group

	HV ≤ 1.0 mL	HV > 1.0 mL	<i>P</i>
Sample size, n (%)	11 (26.2)	31 (73.8)	
Age, mean \pm SD, y	39.5 \pm 23.3	42.6 \pm 19.4	0.672
Sex, n (%)			0.136
Men	5 (45.5)	23 (74.2)	
Women	6 (54.5)	8 (25.8)	
Fractures site, n (%)			0.485
Right	8 (72.7)	18 (58.1)	
Left	3 (27.3)	13 (41.9)	

Table 3. Bivariate Analysis of All Study Variables Versus the Volume of Herniated Orbital Tissue in the MW Fracture Group

	HV ≤ 0.9 mL	HV > 0.9 mL	<i>P</i>
Sample size, n (%)	21 (37.5)	35 (62.5)	
Age, mean \pm SD, y	41.8 \pm 26.9	43.1 \pm 22.9	0.844
Sex, n (%)			1
Men	15 (71.4)	25 (71.4)	
Women	6 (28.6)	10 (28.6)	
Fractures site, n (%)			0.011*
Right	14 (66.7)	10 (28.6)	
Left	7 (33.3)	25 (71.4)	

*Statistically significant ($P < 0.05$).

69.2%, and AUC of 0.956 [95% confidence interval, 0.911–1]).

DISCUSSION

Numerous attempts have been made to clarify the relationship between specific CT characteristics at the time of injury and the degree of PE. With the availability of thin-slice CT and the widespread use of 3-dimensional image analysis software, the relationship between CT imaging characteristics and the degree of PE is being established. Many studies have mentioned the correlation between PE and HV. Jin et al¹³ reported that HV of more than 0.9 mL was associated with PE of 2 mm or more in patients with blowout fractures of the medial orbital wall. In a study of patients with inferior blowout fractures, the HV threshold for visible PE was 1.0 mL.²³ Bouet et al²⁴ assessed the

correlation between HV and incidence of late enophthalmos and found that each 1.0 mL increase in HV was accompanied by a 2 mm increase in enophthalmos.

However, HV measurements can be time-consuming, complicated to perform, and relatively impractical for routine use.²⁰ To determine the HV on CT, the area of herniation must be manually measured on a 2-dimensional image slice and multiplied by the slice thickness; then, these values must be summed across all slices that include the orbit. Although machine-learning algorithms have been developed to automate the measurement of orbital volume, they are not available for use in current versions of radiology imaging software.^{18,25} The aim of this study was to identify a concise, reliable, and clinically applicable method for measuring HV.

We calculated the difference between HV and AVrp/AVqp/AVhe to compare the shape of herniated orbital

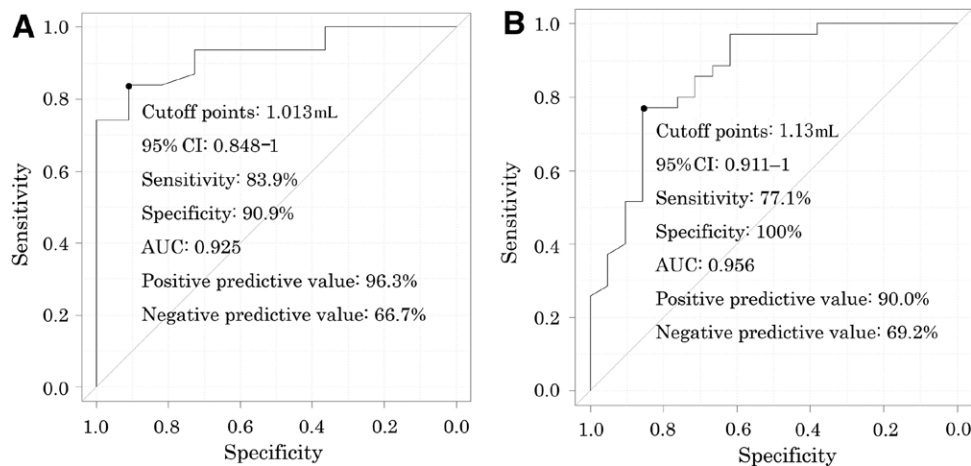


Fig. 5. ROC curves using volume approximated by assuming a hemiellipsoid shape to predict HV in the (A) OF group and (B) MW fracture group. CI, confidence interval.

tissue and the shape of approximated herniated orbital tissue. A difference close to zero indicated that the AV was approximately equal to HV. In both the OF and MW groups, the mean HV–AVhe difference was the closest of the 3 mean differences to 0, suggesting that AVhe provided the closest approximation to the shape of herniated orbital tissue. In both groups, the Pearson correlation analysis showed a positive linear relationship between HV and AVhe.

In the ROC curve analyses, the optimal AVhe cutoff value associated with high HV in the OF group (>1.0 mL) was 1.013 mL. In the MW group, high HV was defined as greater than 0.9 mL, and the optimal AVhe cutoff was 1.13 mL. The AUC values suggested excellent performance in both groups. The positive and negative predictive values in the OF group were 96.3% and 66.7%, respectively; in the MW group, they were 90.0% and 69.2%, respectively.

In summary, this study demonstrated that the approximate volume of herniated orbital contents, calculated as a hemiellipsoidal shape, can serve as a viable substitute for the conventional HV measurement method of manually tracing borders. However, in the MW group, the cutoff values for AVhe differed from HV because the morphology of the MW fracture is presumed to be more complex. This suggests that different cutoff values should be used when using AV as an alternative to HV.

This study demonstrated relatively high specificity and positive predictive values, and low sensitivity and negative predictive values in both groups. Higher specificity and positive predictive values indicate lower false positives. This suggests that patients with high AVhe are more likely to exhibit high HV. However, higher sensitivity and higher negative predictive value are desirable for a screening test. The lower-than-expected negative predictive value could potentially be improved by developing an algorithm that combines several tools, including AVhe.

This study has several limitations. Although the associations of AVrp, AVqp, and AVhe with HV were compared, and the hemiellipsoid shape provided the closest approximation to the shape of herniated orbital tissue, the shape of herniated orbital tissue varies in real-world clinical

practice. Further prospective studies are necessary to demonstrate the clinical usefulness of AVhe. Furthermore, few patients underwent follow-up CT or Hertel exophthalmometry, and a direct comparison between PE and AV was not possible.

The timing of CT scan volumetry is important and controversial. Scolozzi et al²⁶ limited the assessment to the day of injury, whereas Choi et al²⁷ restricted it to within 1 week after injury. Because the degree of edema and fibrosis changes over time after orbital injury, it is necessary to establish standardized criteria for the timing of CT scan volumetry.

CONCLUSIONS

CT image analysis provides valuable data to assist in planning the appropriate treatment for blowout fractures of the orbit. Our simplified method, which approximately calculates the volume of herniated orbital contents in a hemiellipsoid pattern model, proved to be practical, easy, and more reliable than the conventional method.

Takashi Nuri, MD, PhD

Department of Plastic and Reconstructive Surgery
Osaka Medical and Pharmaceutical University
Takatsuki, Osaka 569-8686, Japan
E-mail: takashi.nuri@ompu.ac.jp

DISCLOSURE

The authors have no financial interest to declare in relation to the content of this article.

ACKNOWLEDGMENT

The author would like to thank Dr. Daisuke Nishioka of Japan, Osaka, for giving advice on statistical study design.

REFERENCES

1. Converse JM, Smith B. Enophthalmos and diplopia in fractures of the orbital floor. *Br J Plast Surg*. 1957;9:265–274.
2. Higashino T, Hirabayashi S, Eguchi T, et al. Straightforward factors for predicting the prognosis of blow-out fractures. *J Craniofac Surg*. 2011;22:1210–1214.

3. Burnstine MA. Clinical recommendations for repair of isolated orbital floor fractures: an evidence-based analysis. *Ophthalmology*. 2002;109:1207–1210; discussion 1210.
4. Kim YK, Park CS, Kim HK, et al. Correlation between changes of medial rectus muscle section and enophthalmos in patients with medial orbital wall fracture. *J Plast Reconstr Aesthet Surg*. 2009;62:1379–1383.
5. Ahn HB, Ryu WY, Yoo KW, et al. Prediction of enophthalmos by computer-based volume measurement of orbital fractures in a Korean population. *Ophthal Plast Reconstr Surg*. 2008;24:36–39.
6. Whitehouse RW, Batterbury M, Jackson A, et al. Prediction of enophthalmos by computed tomography after “blow out” orbital fracture. *Br J Ophthalmol*. 1994;78:618–620.
7. Migliori ME, Gladstone GJ. Determination of the normal range of exophthalmometric values for black and white adults. *Am J Ophthalmol*. 1984;98:438–442.
8. Koo L, Hatton MP, Rubin PA. When is enophthalmos “significant?”. *Ophthal Plast Reconstr Surg*. 2006;22:274–277.
9. Osguthorpe JD. Orbital wall fractures: evaluation and management. *Otolaryngol Head Neck Surg*. 1991;105:702–707.
10. Dulley B, Fells P. Long-term follow-up of orbital blow-out fractures with and without surgery. *Mod Probl Ophthalmol*. 1975;14:467–470.
11. Brady SM, McMann MA, Mazzoli RA, et al. The diagnosis and management of orbital blowout fractures: update 2001. *Am J Emerg Med*. 2001;19:147–154.
12. Nikunen M, Rajantie H, Marttila E, et al. Implant malposition and revision surgery in primary orbital fracture reconstructions. *J Craniomaxillofac Surg*. 2021;49:837–844.
13. Jin HR, Shin SO, Choo MJ, et al. Relationship between the extent of fracture and the degree of enophthalmos in isolated blow-out fractures of the medial orbital wall. *J Oral Maxillofac Surg*. 2000;58:617–620; discussion 620.
14. Snell BJ, Flapper W, Moore M, et al. Management of isolated fractures of the medial orbital wall. *J Craniofac Surg*. 2013;24:291–294.
15. Jung S, Lee JW, Kim CH, et al. Postoperative changes in isolated medial orbital wall fractures based on computed tomography. *J Craniofac Surg*. 2017;28:2038–2041.
16. Scawn RL, Lim LH, Whipple KM, et al. Outcomes of orbital blow-out fracture repair performed beyond 6 weeks after injury. *Ophthalmic Plast Reconstr Surg*. 2016;32:296–301.
17. Jackson IT. Classification and treatment of orbitozygomatic and orbitoethmoid fractures. The place of bone grafting and plate fixation. *Clin Plast Surg*. 1989;16:77–91.
18. Basta MN, Rao V, Roussel LO, et al. Refining indications for orbital floor fracture reconstruction: a risk-stratification tool predicting symptom development and need for surgery. *Plast Reconstr Surg*. 2021;148:606–615.
19. Choi A, Sisson A, Olson K, et al. Predictors of delayed enophthalmos after orbital fractures: a systematic review. *Facial Plast Surg Aesthet Med*. 2022;24:397–403.
20. Wevers M, Strabbing EM, Engin O, et al. CT parameters in pure orbital wall fractures and their relevance in the choice of treatment and patient outcome: a systematic review. *Int J Oral Maxillofac Surg*. 2022;51:782–789.
21. De Ruiter BJ, Kotha VS, Lalezar FD, et al. Orbital index: a novel comprehensive quantitative tool for prediction of delayed enophthalmos in orbital floor fracture management. *Plast Reconstr Surg*. 2022;150:625e–629e.
22. Kanda Y. Investigation of the freely available easy-to-use software “EZ” for medical statistics. *Bone Marrow Transplant*. 2013;48:452–458.
23. Alinasab B, Borstedt K-J, Rudstrom R, et al. New algorithm for the management of orbital blowout fracture based on prospective study. *Craniomaxillofac Trauma Reconstr*. 2018;11:285–295.
24. Bouet B, Schlund M, Sentucq C, et al. Radiographic volumetric risk factors for late enophthalmos prediction in orbital blow-out fractures: a retrospective study. *J Craniomaxillofac Surg*. 2022;50:478–484.
25. Jansen J, Schreurs R, Dubois L, et al. Orbital volume analysis: validation of a semi-automatic software segmentation method. *Int J Comput Assist Radiol Surg*. 2016;11:11–18.
26. Scolozzi P, Bachelet J-T, Courvoisier DS. Are inferior rectus muscle displacement and the fracture’s size associated with surgical repair decisions and clinical outcomes in patients with pure blowout orbital fracture? *J Oral Maxillofac Surg*. 2020;78:2280.e1–2280.e10.
27. Choi SH, Kang DH. Prediction of late enophthalmos using pre-operative orbital volume and fracture area measurements in blowout fracture. *J Craniofac Surg*. 2017;28:1717–1720.